Jixin Zhong,[1] Xiaoquan Rao,[1] Zachary Braunstein,[2] Anne Taylor,[3] Vimal Narula,[3] Jeffrey Hazey,[3] Dean Mikami,[3] Bradley Needleman,[3] Jessica Rutsky,[2] Qinghua Sun,[2] Jeffrey A. Deiuliis,[1] Abhay R. Satoskar,[4] and Sanjay Rajagopalan[1]

T-Cell Costimulation Protects Obesity-Induced Adipose Inflammation and Insulin Resistance

Diabetes 2014;63:1289–1302 | DOI: 10.2337/db13-1094

A key pathophysiologic role for activated T-cells in mediating adipose inflammation and insulin resistance (IR) has been recently postulated. However, mechanisms underlying their activation are poorly understood. In this study, we demonstrated a previously unrecognized homeostatic role for the costimulatory B7 molecules (CD80 and CD86) in preventing adipose inflammation. Instead of promoting inflammation, which was found in many other disease conditions, B7 costimulation reduced adipose inflammation by maintaining regulatory T-cell (Treg) numbers in adipose tissue. In both humans and mice, expression of CD80 and CD86 was negatively correlated with the degree of IR and adipose tissue macrophage infiltration. Decreased B7 expression in obesity appeared to directly impair Treg proliferation and function that lead to excessive proinflammatory macrophages and the development of IR. CD80/CD86 double knockout (B7 KO) mice had enhanced adipose macrophage inflammation and IR under both high-fat and normal diet conditions, accompanied by reduced Treg development and proliferation. Adoptive transfer of Tregs reversed IR and adipose inflammation in B7 KO mice. Our results suggest an essential role for B7 in maintaining Tregs and adipose homeostasis and may have important implications for therapies that target costimulation in type 2 diabetes.

Inflammation is widely believed to play a key pathogenic role in the development of obesity-induced insulin resistance (IR) and type 2 diabetes (1–3). While innate immune activation typified by infiltrating macrophages are widely believed to represent important mediators of obesity-related complications, the role of adaptive immune responses is less well characterized. Recent findings suggest that T-cells may play an important role in this process (4–6). Activated $CD8^+$ effector T-cells have recently been shown to promote adipose inflammation by enhancing macrophage recruitment and activation (5,6). The precise mechanisms by which T-cells are activated in obesity remains poorly characterized.

Classically, T-cell activation requires two different types of signals, both of which are delivered by antigen-presenting cells (APCs) (7). The first signal derives from the interaction between T-cell receptor and peptide major histocompatibility complex, whereas the second signal (also called costimulatory signal) is provided by the binding of CD28 to the costimulatory molecules such as CD80 (B7-1) and CD86 (B7-2) (8–11). As the most classical costimulation, B7 is involved in various inflammatory diseases (11–17). Nevertheless, whether B7 molecules play a role in regulation of adipose inflammation in IR is completely unclear. Prevention of B7-mediated costimulation has been suggested to result in impaired T-cell activation, which may be protective in a number of experimental contexts such as experimental allergic encephalomyelitis (11,14), allograft transplantation (12), arthritis (13,16), hypertension (17), and type 1 diabetes (15). In this investigation, we elucidated a homeostatic role of B7-mediated costimulation in diet-induced obesity using CD80/CD86

[1]Division of Cardiology, Department of Medicine, University of Maryland School of Medicine, Baltimore, MD
[2]Davis Heart and Lung Research Institute, The Ohio State University, Columbus, OH
[3]Department of Surgery, The Ohio State University, Columbus, OH
[4]Division of Experimental Pathology, The Ohio State University, Columbus, OH
Corresponding author: Sanjay Rajagopalan, srajagopalan@medicine.umaryland.edu.

Received 12 July 2013 and accepted 8 November 2013.
This article contains Supplementary Data online at http://diabetes.diabetesjournals.org/lookup/suppl/doi:10.2337/db13-1094/-/DC1.

See accompanying article, p. 1179.

double knockout (B7 KO) mice and investigated the relevance of this process in humans with obesity and IR.

RESEARCH DESIGN AND METHODS

Animal Models

All procedures of this study were approved by the Committees on Use and Care of Animals. B7 KO (B6.129S4-Cd80^{tm1Shr} Cd86^{tm2Shr}/J), Foxp3-GFP knock-in (B6.Cg-Foxp3$^{tm2(EGFP)Tch}$/J), and C57BL/6 mice were purchased from The Jackson Laboratory (Bar Harbor, ME). Eight-week-old wild-type (WT) and B7 KO mice were randomized to a normal diet (ND) or a high-fat (HF; 42% calories from fat, Harlan TD.88137) diet for 12 weeks. At sacrifice, mice were fasted overnight and serum was collected for insulin (Crystal Chem, Inc., Downers Grove, IL) and leptin (R&D Systems, Minneapolis, MN) ELISA. Homeostatic model assessment of IR (HOMA-IR) was calculated as follows: HOMA-IR = fasting serum glucose (mg/dL) × fasting plasma insulin (μU/mL) / 405.

Human Subjects

We enrolled prospective obese subjects (BMI >30) as part of research protocol investigating the role of visceral adipose inflammation in obesity. Greater omental adipose tissue was obtained during endoscopic gastric bypass surgery. As controls, human visceral adipose tissue (VAT) was procured during endoscopic repair of hernias from lean controls (BMI <30). Human subcutaneous adipose tissue (SAT) was obtained from patients undergoing lipoaspiration/liposuction as part of a separate institutional review board–approved protocol. The stromal vascular fraction (SVF) from VAT/SAT was isolated by digesting it with 1 mg/mL collagenase type 2 from *Clostridium histolyticum* (Sigma-Aldrich, St. Louis, MO) as described previously (18). All procedures of this study were approved by the Office of Responsible Research Practices, Human Institutional Review Board of The Ohio State University under university protocol 2008H0177. Human informed consent was obtained in writing, and a copy was inserted in the patients' medical records.

Visceral Adipose Assessment and Quantification by Magnetic Resonance Imaging

Magnetic resonance imaging (MRI) was performed to assess degree of adiposity. After 12 weeks of HF diet, MRI was performed on a 9.4 T Bruker BioSpin system equipped with ParaVision 4.0 software as previously described (19). A spin echo sequence (repetition time 920 ms, echo time 12 ms, in-plane resolution 256 × 256 μm; 2, 4 averages) was used to acquire 50 transversal, 1-mm thick slices that covered from the top of the kidneys to the hind legs. Fat quantification analysis was performed using OsiriX software (OsiriX Foundation, Geneva, Switzerland). Thresholding technique was applied to all images to separate fat and water signal.

Induction of Bone Marrow–Derived Dendritic Cells and Bone Marrow–Derived Macrophages

Bone marrow–derived dendritic cells (BMDCs) were generated as previously described (20). For the induction of bone marrow–derived macrophages (BMMs), bone marrow cells were cultured in RPMI-1640 suspended with 10% FBS and 10 ng/ml recombinant mouse M-CSF (R&D Systems). Media were replaced every 2 days. Adherent cells (BMMs) were collected for experiment at day 7.

Intraperitoneal Glucose Tolerance Test and Insulin Tolerance Test

Intraperitoneal glucose tolerance tests (IPGTTs) and insulin tolerance tests (ITTs) were performed following 12 weeks of diet feeding as detailed previously with minor modifications (21). For IPGTT, mice were weighed and baseline blood glucose was determined after overnight fasting (16–18 h) with free access to water. Animals were then intraperitoneally injected with 2 g/kg D-glucose. Blood glucose was detected 30, 60, 90, and 120 min after the glucose injection by using a Contour blood glucose meter (Bayer, Pittsburgh, PA). For ITT, body weight and baseline blood glucose were measured after 4 h of fasting. Mice were then intraperitoneally injected with 0.75 units/kg insulin, and blood glucose was detected at 30, 60, 90, and 120 min.

Flow Cytometry

All antibodies used in flow cytometry were purchased from BioLegend (San Diego, CA) or BD (San Jose, CA). Cells were stained with indicated antibodies as described previously (18) and then analyzed on a BD LSR II cytometer. For intracellular staining of Foxp3, cells were incubated with antibodies against surface maker at 4°C for 15 min. After a wash with PBS, cells were then fixed and permeabilized using a Foxp3 staining kit (BioLegend) as instructed by the manufacturer.

Real-Time PCR

Total RNA were isolated from epididymal fat using Trizol Reagent (Life Technologies, Grand Island, NY). cDNA were synthesized from mRNA using a high-capacity cDNA reverse transcriptase kit (Life Technologies) according to the manufacturer's instruction. Real-time PCR was performed using a LightCycler 480 SYBR Green I Master kit (Roche, Indianapolis, IN). 18s rRNA was used as internal control. Primers are listed in Supplementary Table 1.

ELISA

Serum insulin level and leptin level were measured using an ultra-sensitive mouse insulin ELISA kit (Crystal Chem, Inc.) and a quantikine mouse leptin immunoassay kit (R&D Systems) as instructed by the manufacturer.

Western Blot Detection

Total proteins were prepared from adipose tissue using M-PER mammalian protein extraction reagent (Thermo Scientific, Waltham, MA) supplemented with protease inhibitor cocktail (Sigma-Aldrich). Western blot analysis was carried out as reported by probing the blots with an indicated primary Ab (Santa Cruz, CA) followed by a horseradish-peroxidase-conjugated secondary antibody (Santa Cruz, CA). The reactive bands were visualized using an ECL Plus Western Blotting kit (Pierce, Rockford, IL).

Macrophage/T-Cell Coculture

Regulatory T-cells (Tregs) were isolated from the lymph nodes and spleen of Foxp3-GFP knock-in mice by flow sorting. $CD4^+$ GFP^+ natural Tregs and $CD4^+$ GFP^- naïve T-cells (Tn) were cocultured with BMMs at the concentration of 1×10^6/mL for 5 days. Cells were then harvested for the detection of macrophage polarization and Treg proliferation. For cell proliferation assay, Tregs were labeled with CellTrace violet stain (CellTrace Violet Cell Proliferation Kit, Life Technologies) before coculture according to the manufacturer's instruction. Fluorescence intensity was analyzed on an LSR II flow cytometer, and proliferation was evaluated by the percentage of divided cells (with lower fluorescence intensity). For the analysis of Treg development, thymocytes were isolated from Foxp3-GFP knock-in mice and cocultured with BMMs or BMDCs derived from WT or B7 KO mice. Treg percentage in thymocytes was evaluated after 5 days of coculture by flow cytometry.

Treg Adoptive Transfer

For the adoptive transfer study, natural Treg and $Foxp3^-$ Tn were prepared from Foxp3-GFP knock-in mice by flow sorting. Treg or Tn (0.5×10^6/mouse) were then suspended in 200 μL 1 × PBS and adoptive transferred into B7 KO mice by intravenous injection. The day after first injection, mice were fed an HF diet for 12 weeks. The adoptive transfer was performed every 2 weeks until sacrifice.

Statistical Analysis

All data are presented as mean ± SEM. A P value of <0.05 was considered statistically significant. GraphPad Prism 4 was used for statistical analysis using Student t test or one-way ANOVA and Bonferroni post hoc test where appropriate.

RESULTS

Reduced CD80 and CD86 Expression in Adipose Tissue Macrophage From Obese Humans and Mice

To investigate a potential role for costimulatory molecules CD80 (B7-1) and CD86 (B7-2) in obesity-induced IR, VAT and SAT isolated from lean and obese humans were used for flow cytometric detection of CD80 and CD86. Supplementary Table 2 provides baseline metabolic data of patients recruited to the study. Expression of CD80 and CD86 was lower in monocyte/macrophage lineage cells ($CD45^+CD14^+$) and mature macrophages (defined as $CD45^+CD11b^+$) in VAT from obese patients compared with that of lean (BMI <30) controls (Fig. 1*A–D*). Similarly, CD80 and CD86 expression was lower in $CD45^+CD14^+$ and $CD45^+CD11b^+$ cells from SAT of obese subjects (BMI ≥ 30) compared with lean controls (BMI <30) (Fig. 1*E–H*). CD80 and CD86 expression on adipose tissue macrophage (ATM) in VAT was negatively correlated with HOMA-IR, suggesting a potential role of CD80 and CD86 in the pathogenesis of obesity-induced IR (Fig. 1*H* and *I*). Consistent with human data, expression of CD80 and CD86 on ATM of mice fed an HF diet was lower compared with ND-fed mice (data not shown).

Deficiency of B7 Exacerbates IR Despite Less Adiposity

To investigate the involvement of costimulatory molecules CD80 and CD86 in obesity and IR, WT and B7 KO (CD80 and CD86 double knockout) mice were fed an HF diet or ND for a duration of 12 weeks. There were no significant differences in body weight between WT and B7 KO fed ND. In response to HF diet, both WT and B7 KO mice significantly gained weight compared with ND-fed animals, but the degree of body weight gain was identical in B7 KO and WT animals (48.9 ± 1.2 vs. 49.0 ± 1.3 g; $P > 0.05$) (Fig. 2*A*). B7 KO mice had significantly lower epididymal fat after 12 weeks of HF diet feeding (1.31 ± 0.04 vs. 0.92 ± 0.06 g for WT vs. B7 KO; $P = 0.005$) (Fig. 2*B*). MRI analysis of VAT content demonstrated similar findings. Abdominal fat analysis by MRI (visceral and subcutaneous) demonstrated a reduction in both compartments in B7 KO mice (Fig. 2*C*). Liver weight was higher in B7 KO mice on HF diet (3.92 ± 0.14 vs. 4.38 ± 0.08 g for WT vs. B7 KO; $P = 0.02$) (Fig. 2*D*). Hepatic triglyceride and cholesterol was significantly increased in response to HF diet but without significant differences between WT and B7 KO mice (Fig. 2*E*).

Figure 2*F* and *G* depicts insulin and glucose homeostasis measures as evidenced by IPGTT and ITT. B7 KO mice exhibited significantly worse fasting glucose levels even under ND conditions. Fasting blood glucose levels significantly increased after 12 weeks of HF diet in both WT and B7 KO mice. Overnight fasting blood glucose levels in B7 KO mice fed an HF diet were higher than WT HF-fed animals (Fig. 2*H*) (ND 78.4 ± 1.5 vs. 94 ± 7.7 mg/dL, $n = 10$, $P = 0.041$; HF 107.6 ± 4.7 vs. 127 ± 7.9 mg/dL, $n = 10$, $P = 0.042$). Fasting insulin levels were significantly higher in B7 KO mice on both ND and HF diet compared with WT mice on corresponding diets (Fig. 2*I*) (ND 0.46 ± 0.13 vs. 0.96 ± 0.11 ng/mL, $P = 0.024$; HF 1.27 ± 0.10 vs. 1.93 ± 0.04 ng/mL, $P = 0.027$). HOMA-IR values were significantly higher in the B7 KO mice on both ND and HF diet (Fig. 2*J*). There was an increase in serum leptin level upon HF diet feeding. However, no significant difference in leptin levels was observed between WT and B7 KO mice (Fig. 2*K*).

Defective B7-Mediated Costimulation Affects Adipose Inflammation and T-Cell Activation in Circulation

We next evaluated the contribution of B7 to inflammation in circulation and adipose tissue in diet-induced obesity. We first confirmed the absence of CD80 and CD86 expression in splenic and peritoneal macrophages in B7 KO mice (data not shown). As depicted in Fig. 3*A* and *B*, comparable amounts of macrophages ($CD11b^+$ $F4/80^+$) and total T-cells ($CD45^+CD3^+$) were detected in the spleen of WT and B7 KO mice. However, B7 KO mice had reduced $CD4^+$ T-cells and increased $CD8^+$ T-cells in the spleen (Fig. 3*C*). Further analysis demonstrated that B7 KO

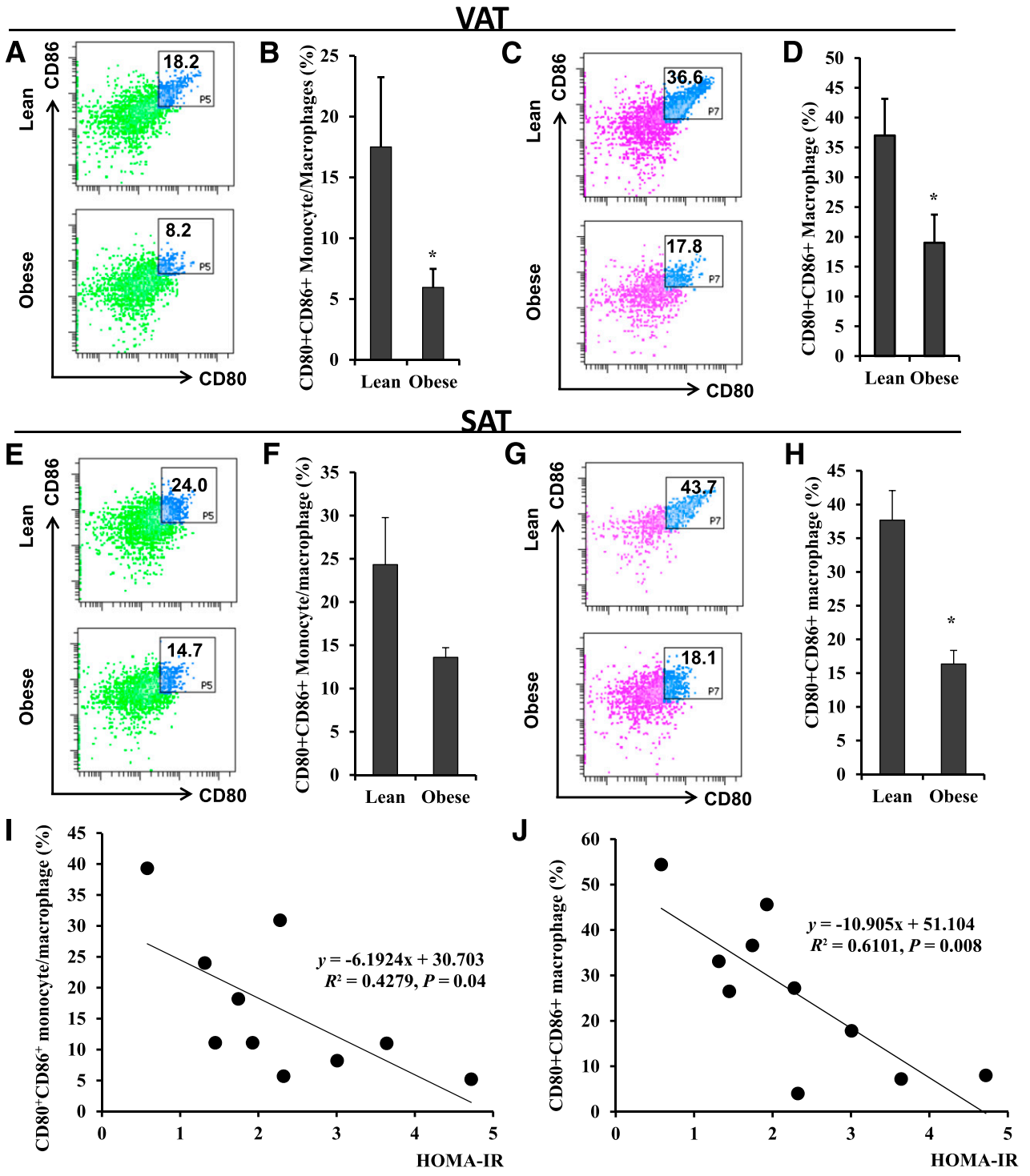

Figure 1—Reduced CD80 and CD86 expression on ATM of obese humans. *A–D*: SVF was isolated from VAT of lean humans undergoing inguinal herniorrhaphy (BMI <30) and obese patients undergoing bariatric intervention (BMI ≥30), followed by flow cytometric analysis. $CD45^+CD14^+$ monocyte/macrophage ([*A*] representative images and [*B*] statistical analysis) or $CD45^+CD11b^+$ mature macrophage ([*C*] representative images and [*D*] statistical analysis) were gated for the detection of CD80 and CD86. *E–H*: SVF was isolated from SAT of obese (BMI <30) and lean (BMI ≥30) humans undergoing lipoaspiration/liposuction followed by flow cytometric analysis. $CD45^+CD14^+$ monocyte/macrophage ([*E*] representative images and [*F*] statistical analysis) or $CD45^+CD11b^+$ mature macrophage ([*G*] representative images and [*H*] statistical analysis) were gated for the detection of CD80 and CD86. Associations of HOMA-IR with $CD80^+$ $CD86^+$ (*I*) monocyte/macrophage or (*J*) mature macrophage in VAT was shown. $n = 10$. *$P < 0.05$.

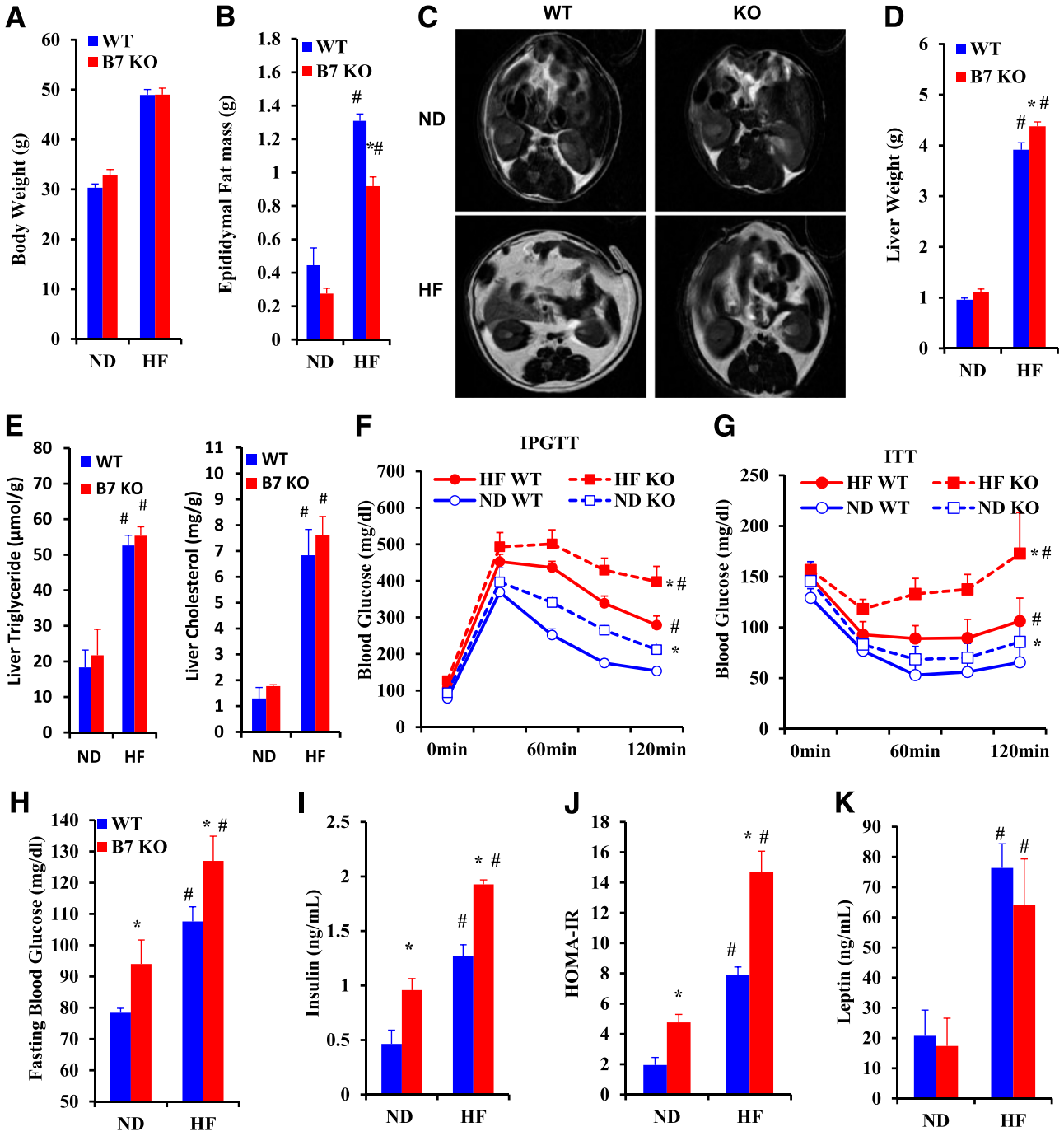

Figure 2—B7 deficiency reduces visceral fat mass, but exacerbates diet-induced IR. WT and CD80$^{-/-}$ CD86$^{-/-}$ (B7 KO) mice were fed an ND or HF diet. *A*: Body weight of the mice was measured after 12 weeks of diet feeding. The adiposity was evaluated by (*B*) epididymal fat weight and (*C*) MRI analysis. (*D*) Liver weight and (*E*) hepatic lipid levels (*left*, triglyceride; *right*, cholesterol) were examined. (*F*) IPGTT and (*G*) ITT on WT and B7 KO mice were performed after 12 weeks of diet feeding (n = 8). *H*: Fasting blood glucose was measured after 16 h of overnight fasting. Plasma was collected after 16 h of fasting and used for ELISA detection of insulin and leptin. HOMA-IR was calculated as follows: HOMA-IR = fasting serum glucose (mg/dL) × fasting plasma insulin (μU/mL) / 405. (*I*) Fasting insulin, (*J*) HOMA-IR, and (*K*) leptin were shown. *P < 0.05 compared with WT; #P < 0.05 compared with ND; n = 10–12 per group.

mice had decreased populations of activated CD4$^+$ T-cells (less expression of T-cell activation marker CD44 and CD69) in the spleen compared with WT mice (Fig. 3*D*–*G*). However, no significant differences were found in splenic CD8$^+$ T-cells (Fig. 3*D*–*G*), suggesting a reduced circulating CD4 T-cell activation in B7 KO mice. In contrast, innate adipose inflammation was enhanced in B7 KO mice. Increased CD11b$^+$F4/80$^+$ macrophages and expression of

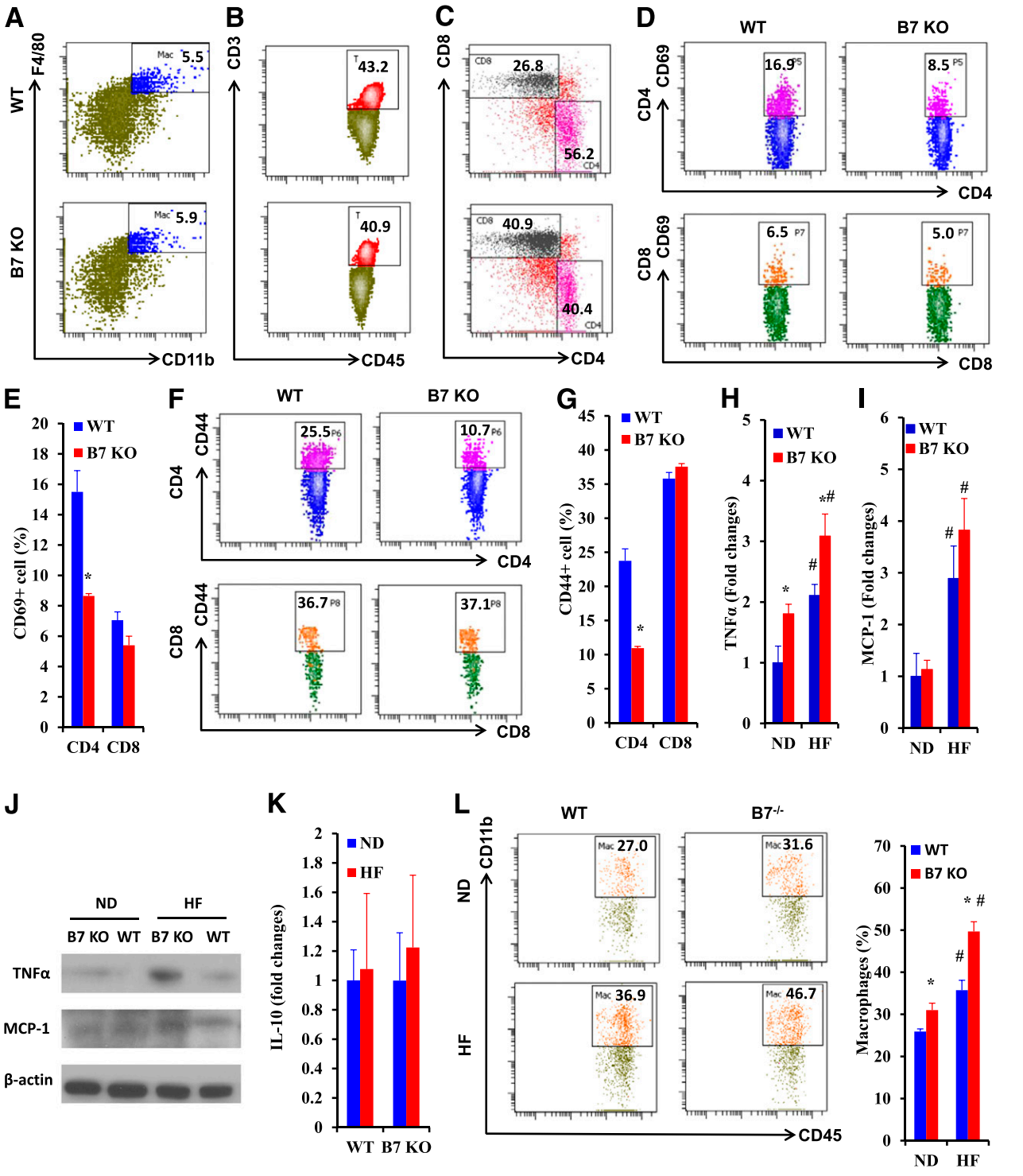

Figure 3—Lack of B7 in mice promotes adipose inflammation despite lower activation of T-cells in circulation. Splenocytes harvested from WT and CD80$^{-/-}$ CD86$^{-/-}$ (B7 KO) mice were used to analyze immune cell populations (n = 12 per group). *A*: CD45$^+$ inflammatory cells were gated for the analysis of macrophages. CD11b$^+$F4/80$^+$ cells in WT and B7 KO mice were shown. *B*: CD45$^+$ inflammatory cells were gated, and total T-cells (CD3$^+$) were analyzed. *C*: Splenic T-cells (CD45$^+$CD3$^+$) were gated for helper T-cells (CD4$^+$) and cytotoxic T-cells (CD8$^+$). *D–G*: Splenic CD4$^+$ and CD8$^+$ T-cells were then gated for the analysis of T-cell activation marker CD69 ([*D*] representative images and [*E*] statistical analysis) and CD44 ([*F*] representative images and [*G*] statistical analysis). *H–J*: WT and B7 KO mice were fed an HF diet or ND for 12 weeks. Epididymal fat was isolated for the real-time PCR and Western blot analysis of (*H*) TNFα, (*I*) MCP-1, and (*K*) interleukin-10 expression. *L*: SVF isolated from epididymal fat was used for the analysis of macrophage (CD45$^+$ CD11b$^+$) infiltration in adipose tissue (*left*, representative images; *right*, statistical analysis). Three independent experiments were performed and consistent results were obtained. *P < 0.05 compared with WT; #P < 0.05 compared with ND; IL-10, interleukin-10; Mac, macrophages; T, T-cells.

tumor necrosis factor-α (TNFα) were observed in VAT of B7 KO mice (Fig. 3*H–J*). There was an approximately two-fold increase of TNFα in the VAT of WT mice fed an HF diet compared with ND, with a further increase seen in B7-deficient mice fed an HF diet (Fig. 3*H* and *J*). Monocyte chemotactic protein-1 (MCP-1) level in mice fed an HF diet increased 1.9-fold compared with that of ND mice. However, no significance was observed between WT and B7 KO mice (Fig. 3*I* and *J*). No significant difference in expression of interleukin-10, an anti-inflammatory cytokine, was observed (Fig. 3*K*). The percentage of $CD45^+CD11b^+$ macrophages increased in VAT of HF WT mice compared with that of ND WT mice (increased from 27 to 36.9%) (Fig. 3*J*). Compared with WT mice, B7 KO mice had a higher level of macrophage infiltration under both ND and HF diet conditions (Fig. 3*L*). Consistent with these findings, there was an enhanced hepatic inflammation in B7 KO mice, as evidenced by increased TNFα expression and immune cell infiltration (data not shown).

Loss of B7-Mediated Costimulation Reduces Tregs Both Systemically and Locally in Adipose Tissue

Prior studies have highlighted the importance of Tregs in obesity and IR, with studies suggesting reduced local differentiation of Tregs as a critical determinant of heightened innate immune responses (4–6). Since CD28 and CTLA-4 have been implicated in Treg development, we reasoned that one mechanism for heightened innate immune activation in adipose tissue may involve Treg pathways. As shown in Fig. 4*A*, $CD3^+$ T-cell infiltration in VAT increased in response to HF diet. However, $CD3^+$ T-cells decreased in B7 KO mice in both ND and HF groups. CD4 significantly decreased in the visceral fat of B7 KO mice. CD8 also slightly decreased in B7 KO mice (data not shown). We next quantified Foxp3, a Treg-restricted transcription factor, in VAT of both WT and B7 KO mice in response to HF diet. Consistent with prior studies, Foxp3 expression decreased in the VAT of HF-fed WT mice compared with ND-fed WT mice (Fig. 4*B*). Foxp3 gene expression was, however, markedly decreased in the VAT of B7 KO mice compared with that of WT mice under both ND and HF diet conditions (Fig. 4*B*). Flow cytometry confirmed the decrease of Treg in VAT of B7 KO mice (Fig. 4*C*). Treg numbers were also decreased in the spleen, blood, and lymph nodes of B7 KO mice (Fig. 4*D*), suggesting a systemic reduction of Tregs in B7 KO mice. To further confirm the relation between ATM B7 expression and Treg in human, human VAT samples were analyzed for the cytometric detection of Treg ($CD4^+Foxp3^+CD25^+$) and B7-expressing ATMs ($CD80^+CD86^+CD11b^+$). As shown in Fig. 4*E*, there was a positive correlation between B7 expression on ATM and Treg percentage in VAT (P = 0.01).

Costimulation Mediated by B7 Molecules Promotes Proliferation of Treg

We next investigated the requirement of B7-mediated costimulation in Treg expansion. Treg cells were flow sorted from Foxp3-GFP knock-in mice and fluorescently labeled using a CellTrace violet cell proliferation kit. Labeled Treg cells were then cocultured with BMMs from WT or B7 KO mice for 5 days, and proliferation of Treg was evaluated by the intensity of the fluorescence (Fig. 5*A*). As demonstrated in Fig. 5*B* and *C*, loss of B7-mediated costimulation significantly impaired the ability of macrophages to stimulate Treg proliferation (5.4 ± 0.3 vs. 2.3 ± 0.4%; $P < 0.05$). To investigate the suppressive function of Treg cocultured with $B7^{-/-}$ macrophages, WT splenic T-cells were cocultured with Treg cells harvested from the coculture system depicted in Fig. 5*A*. After 5 days of coculture, T-cells were collected for flow cytometric detection of T-cell activation marker CD44 and CD69. As shown in Fig. 5*D* and *E*, Treg cells cocultured with $B7^{-/-}$ macrophages were less effective in suppressing T-cell activation.

Disruption of B7 Impairs Ability of Dendritic Cell/Macrophage to Educate Thymocytes and Convert $Foxp3^-$ T-Cells to Treg

Professional APCs, including dendritic cells and macrophages, are required for the development of Treg in thymus and peripheral tissues (22–25). To investigate the role of B7 molecules in Treg development, thymocytes from Foxp3-GFP knock-in mice were cocultured with WT or $B7^{-/-}$ BMMs. After 5 days of coculture, $CD4^+$ cells were gated for the detection of Treg (GFP^+) population (Fig. 6*A*). Smaller amounts of Treg cells were present in thymocytes cocultured with $B7^{-/-}$ BMMs (19.6 ± 2.2 vs. 12.2 ± 1.1% for WT vs. B7 KO; $P < 0.05$) (Fig. 6*B* and *C*). Similarly, $B7^{-/-}$ BMDCs have a reduced ability to drive Treg development (Fig. 6*D* and *E*). It has been shown that $Foxp3^-$ T-cells can be converted into $Foxp3^+$ Treg cells (26). To investigate whether B7 molecules play a role in the conversion of $Foxp3^-$ T-cells to Treg, $Foxp3^-$ T-cells were sorted from Foxp3-GFP knock-in mice and cocultured with WT or $B7^{-/-}$ BMDCs. As a result, $B7^{-/-}$ BMDCs were less potent in converting $Foxp3^-$ T-cells to $Foxp3^+$ Treg cells (11.1 ± 0.3 vs. 5.9 ± 1.2% for WT vs. B7 KO; $P < 0.05$) (Fig. 6*F* and *G*).

Enhanced Adipose Inflammation in B7 KO Mice Is a Result of Reduced Treg

To confirm the involvement of Treg in preventing adipose inflammation, human VAT samples were used for flow cytometric detection of Treg ($CD4^+Foxp3^+CD25^+$) and $CD11c^+CD11b^+$ cells. As depicted in Fig. 7*A*, there was a negative association between Treg and $CD11c^+CD11b^+$ cells in VAT (R^2 = 0.29; P = 0.048). To further investigate whether reduced Treg in B7 KO mice is responsible for heightened adipose innate immune inflammation and IR, the effect of Treg on macrophage activation was examined. As depicted in Fig. 7*B* and *C*, Treg reduced $CD11c^+CD11b^+$ cells (72.3 ± 1.9 vs. 51.2 ± 0.8% for WT vs. B7 KO; $P < 0.05$), a subpopulation that plays an important role in adipose inflammation and IR (27). Consistently, higher percentages of $CD11c^+CD11b^+$ cells were observed in B7 KO mice on both ND and HF diet (Fig. 7*D*).

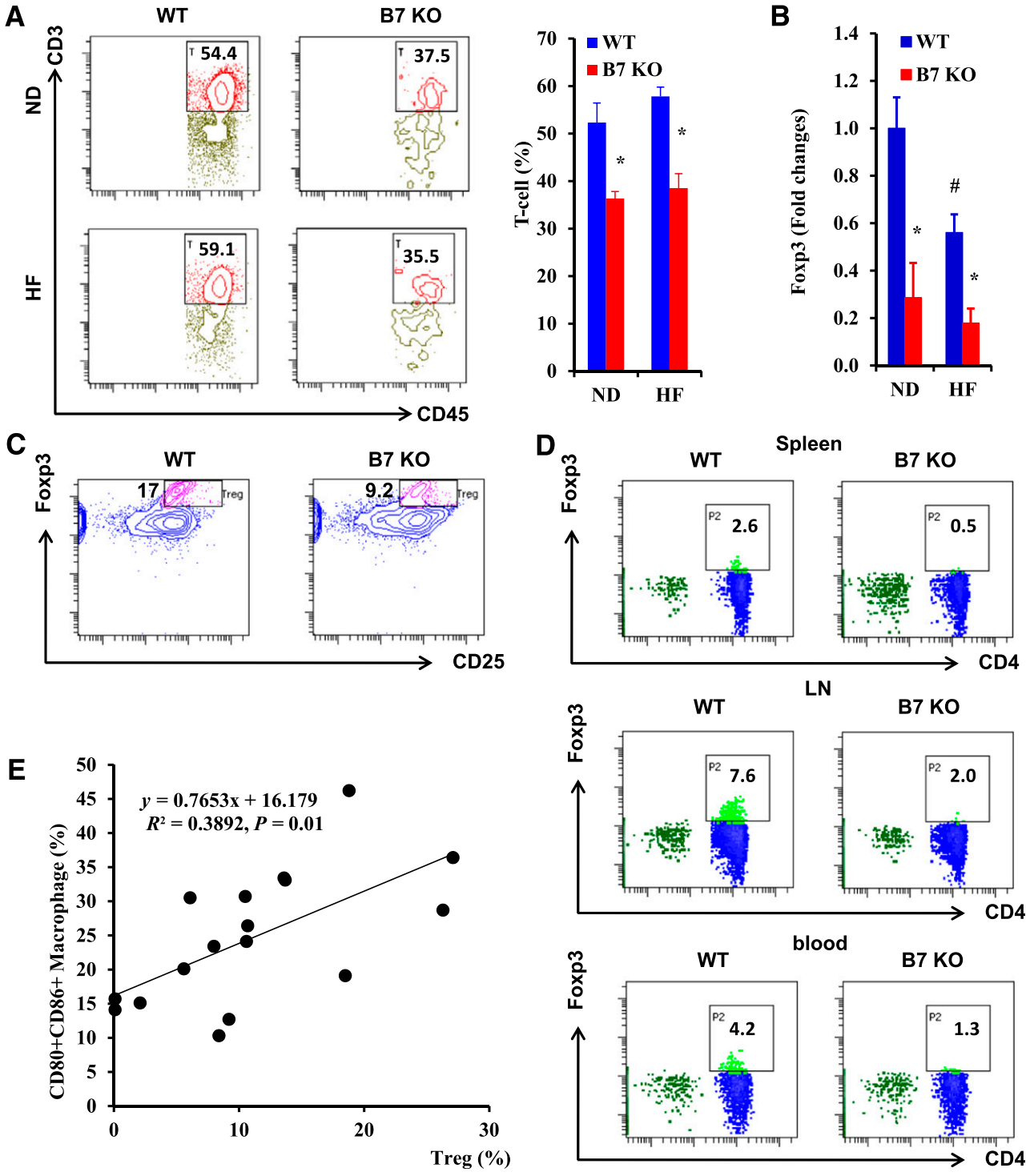

Figure 4—Loss of B7 reduces Treg in mice. *A*: WT and B7 KO mice were fed an HF diet or ND for 12 weeks. SVF was isolated from epididymal fat and used for the flow cytometric detection of T-cells ($CD45^+$ $CD3^+$; *left*, representative images; *right*, statistical analysis). *B*: Foxp3 expression in VAT was detected by real-time PCR. *C*: Epididymal fat from 8-week-old WT and B7 KO male mice (on ND) was used for the isolation of SVF. SVF was then used for flow cytometric detection of Treg using a Foxp3 staining kit. $CD4^+$ T-cells were gated, and Tregs ($CD25^+$ $Foxp3^+$) in SVF were examined. *D*: Tregs ($CD4^+Foxp3^+$) in spleen, blood, and lymph node were detected in WT and B7 KO mice. *E*: SVF isolated from human VAT was stained with anti-CD4, anti-CD25, anti-Foxp3, anti-CD11b, anti-CD80, and anti-CD86 antibodies, followed by flow cytometric analysis. $CD4^+$ cells were gated for the analysis of Tregs ($Foxp3^+CD25^+$), and macrophages ($CD11b^+$) were gated for the analysis of B7 expression ($CD80^+CD86^+$). Correlation between B7 expression on ATM and Treg percentage were examined. $n = 14$. LN, lymph node; $^*P < 0.05$ compared with WT; $\#P < 0.05$ compared with ND; T, T-cell.

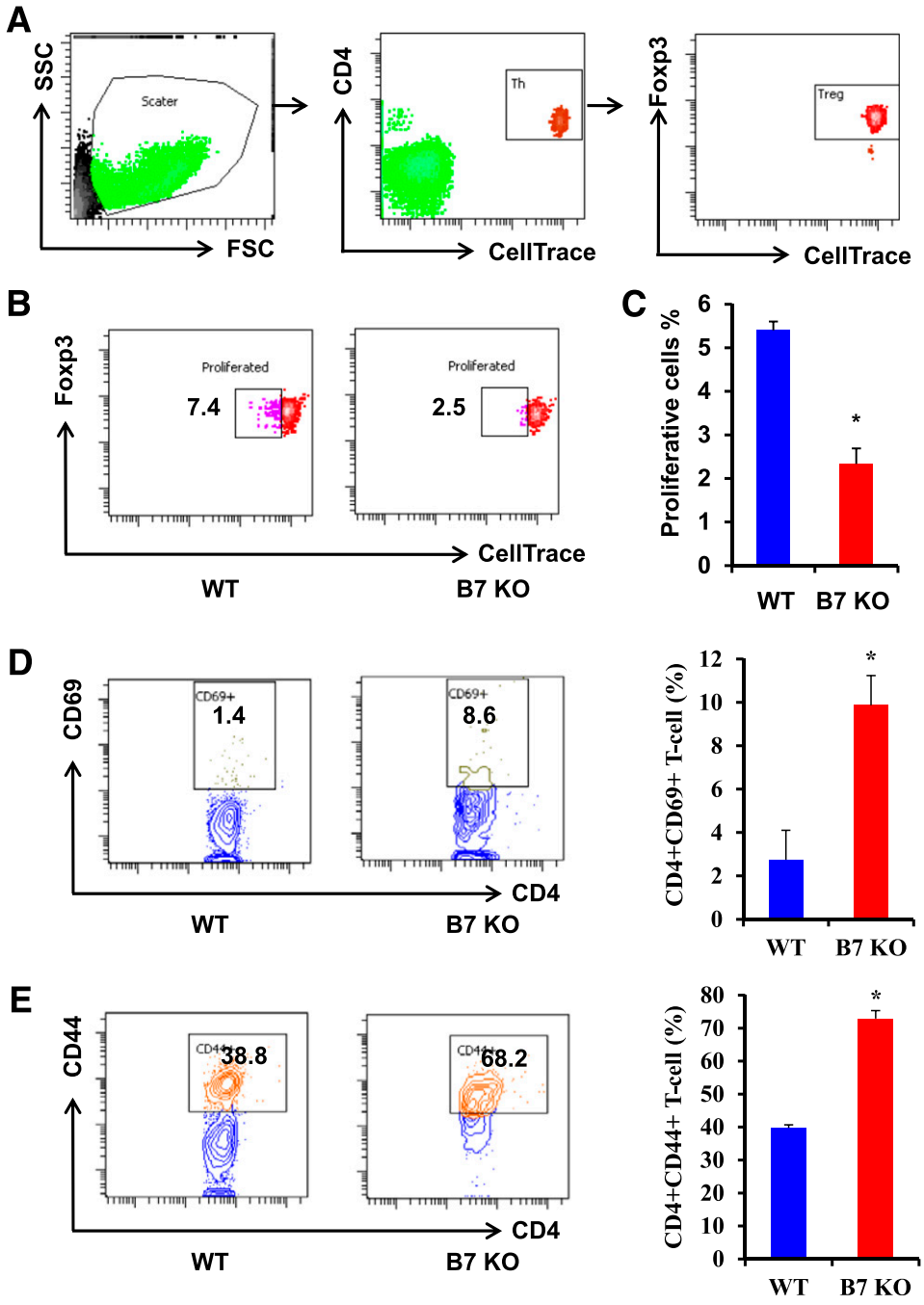

Figure 5—B7-mediated costimulation promotes Treg proliferation. *A–C*: Tregs were isolated from Foxp3-GFP knock-in mice using flow sorting, labeled with CellTrace violet, and then cocultured with WT or B7 KO BMMs. Cells were collected for detection of proliferation after 5 days. *A*: In the gating strategy, leukocytes were gated according to forward scatter and side scatter. Tregs ($CD4^+CellTrace^+Foxp3^+$) were then gated for the analysis of CellTrace intensity. *B*: Proliferated Tregs with a lower fluorescence intensity were evaluated using flow cytometry. Representative images show lower proliferation of Treg when cocultured with B7 KO BMMs. *C*: Statistical result of Treg proliferation. *D* and *E*: Tregs cocultured with WT or B7 KO BMMs were used for suppression assay. Tregs harvested from coculture system were then cultured with WT splenocytes for 5 days. Cells were collected for the analysis of T-cell activation markers (*D*) CD69 and (*E*) CD44. Representative images (*left*) and statistical result (*right*) were shown. *$P < 0.05$; FSC, forward scatter; SSC, side scatter; Th, $CD4^+$ cells.

To further confirm whether enhanced IR in B7 KO mice is dependent on the decrease of Tregs, $CD4^+GFP^+$ Treg or $CD4^+GFP^-$ Tn cells from Foxp3-GFP knock-in mice were adoptively transferred into B7 KO mice (once every other week) and fed an HF diet. After 12 weeks of HF diet feeding, transferred Treg ($CD4^+GFP^+$ cells) presented in both circulation (data not shown) and VAT of mice injected with Treg (Fig. 8*A*). No significant changes in

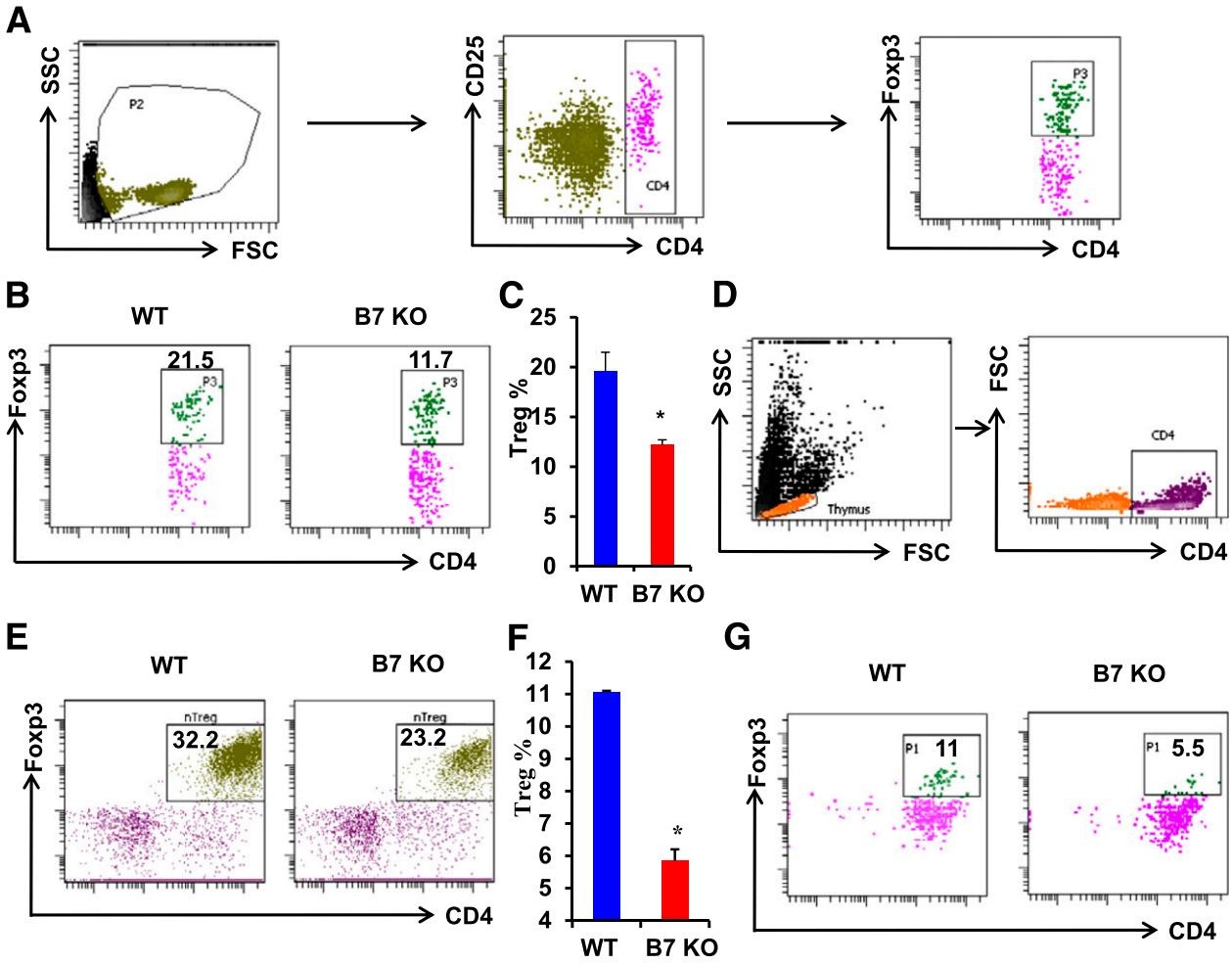

Figure 6—Loss of B7 impairs the ability of APCs to induce Treg. *A*–*C*: WT or B7 KO BMMs were cocultured with thymocytes isolated from Foxp3-GFP knock-in mice in the presence of 2 ng/mL transforming growth factor (TGF)-β. Cells were collected for flow cytometric analysis after 5 days' coculture. *A*: For the gating strategy, cells were first gated for leukocytes according to forward scatter and side scatter, and then $CD4^+$ cells were gated for the analysis of Foxp3 expression. $Foxp3^+$ Tregs in thymocytes cocultured with WT or B7 KO BMMs were shown ([*B*] representative images and [*C*] statistical analysis). *D* and *E*: WT or B7 KO BMDCs were cocultured with thymocytes isolated from Foxp3-GFP knock-in mice in the presence of 2 ng/mL TGF-β. Cells were collected for flow cytometric analysis of Treg. Thymocytes were first gated according to forward scatter and side scatter. *D*: $CD4^+$ cells were then gated for the analysis of Treg. *E*: Tregs differentiated from thymocytes cocultured with B7 KO BMDCs were shown. *F* and *G*: $Foxp3^-$ Tn were sorted from Foxp3-GFP knock-in splenocytes and cocultured with WT or B7 KO BMDCs in the presence of 2 ng/mL TGF-β. Tregs converted from Tn were shown ([*F*] bar graph and [*G*] representative images). Three independent experiments were performed and consistent results were obtained. $^*P < 0.05$; $n = 5$–7 per group; FSC, forward scatter; nTreg, $CD4^+GFP^+$ cells; SSC, side scatter.

body weight and visceral fat weight were observed (data not shown). There was an ~2.1-fold increase of Foxp3 expression in the VAT of mice transferred with Treg (Fig. 8*B*). Macrophage infiltration and its classical activation were reduced by exogenous Treg transfer (Fig. 8*C* and *D*). Adoptive transfer of Treg also restored insulin sensitivity in B7 KO mice, as evidenced by improved IPGTT and ITT (Fig. 8*E* and *F*).

DISCUSSION

In this article, we demonstrate a previously unrecognized homeostatic function of costimulation in preserving Treg numbers and modulating innate immune responses. The main novel findings of our work are as follows: *1*) expression of B7-1 and B7-2 (CD80 and CD86) on APCs in both VAT and SAT is reduced in diet-induced obesity in mice and human obesity; *2*) loss of B7-mediated costimulation exacerbates diet-induced IR despite lower visceral adiposity in both ND and HF diet contexts; *3*) contrary to the expected reduction in innate immune activation, genetic deletion of B7 promoted adipose inflammation; *4*) B7-mediated costimulation is required for the development and expansion of Treg; and *5*) adoptive transfer of Tregs restores insulin sensitivity in response to genetic B7 deficiency.

Recent studies have suggested a critical role of T-cells in mediating obesity-induced adipose inflammation (4–6). Inflamed adipocytes and activated T-cells in the VAT are

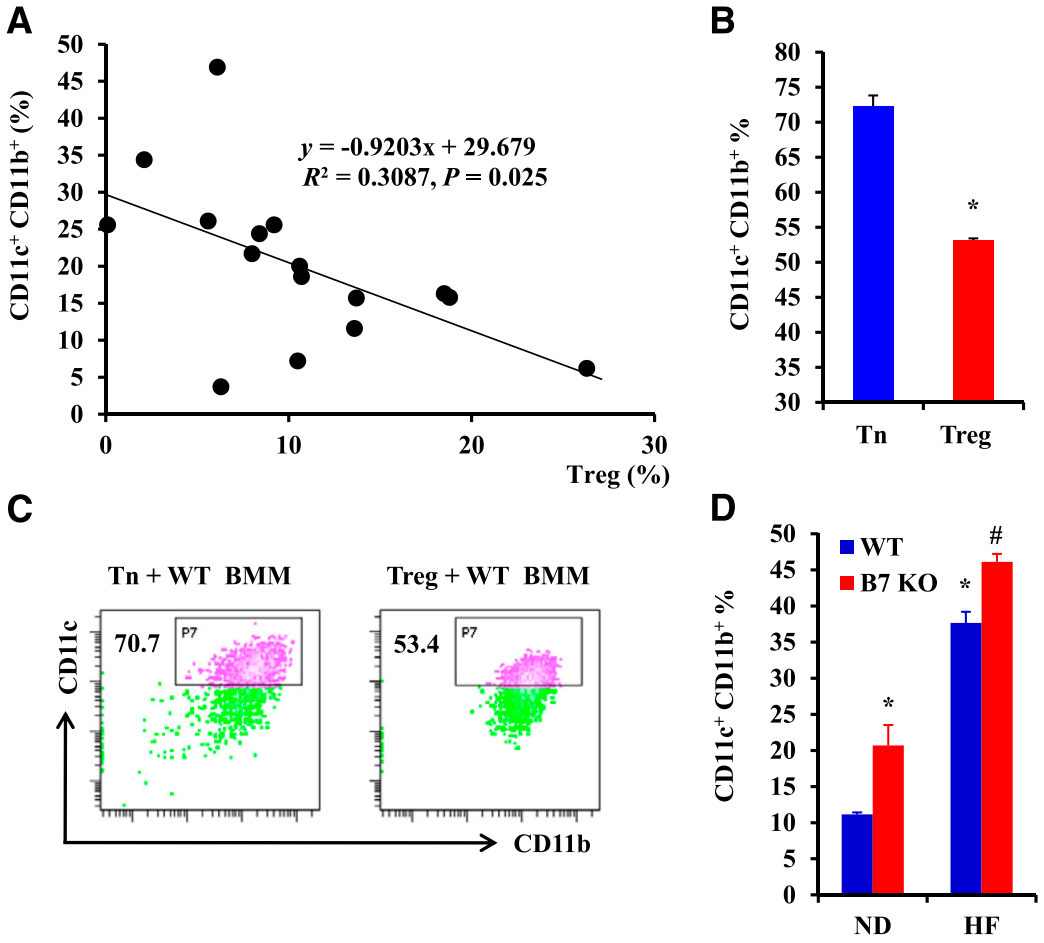

Figure 7—Treg suppresses classical activation of macrophages. *A*: SVF isolated from human VAT was stained with anti-CD4, anti-CD25, anti-Foxp3, anti-CD11b, and anti-CD11c antibodies, followed by flow cytometric analysis. $CD4^+$ cells were gated for the analysis of Tregs ($Foxp3^+CD25^+$), and macrophages ($CD11b^+$) were gated for the analysis of $CD11c^+CD11b^+$ cells. Correlations between $CD11c^+$ $CD11b^+$ cells and Treg in VAT were examined. $n = 14$. *B* and *C*: Treg or Tn were isolated from Foxp3-GFP knock-in mice using flow sorting. Treg or Tn were then cocultured with WT BMMs for 5 days, followed by flow cytometric analysis of $CD11c^+$ $CD11b^+$ cells ([*B*] statistical analysis and [*C*] representative images). *D*: SVF isolated from WT or B7 mice fed a normal chow or HF diet was used for flow cytometric analysis of $CD11c^+$ $CD11b^+$ cells. $^*P < 0.05$ compared with WT; $\#P < 0.05$ compared with ND.

widely believed to secrete a number of chemokines to recruit macrophages to adipose tissue. However, the underlying mechanisms for impaired T-cell homeostasis in obesity is poorly understood.

B7/CD28-mediated costimulatory signal is required for activation and effector function of T-cells (7). Typically, engagement of the T-cell receptor in the absence of costimulation leads to suboptimal T-cell stimulation, anergy, and apoptosis. CD28 is constitutively expressed by naïve T-cells and binds to the ligands CD80 (B7-1) and CD86 (B7-2), expressed on the surface of professional APCs. Whether B7 molecules are involved in obesity and IR is completely unclear. The contribution of costimulation has been widely studied in the context of autoimmune disease where, in general, it has been shown to play a facilitatory role in promoting inflammation. Approaches to decrease costimulation such as genetic or immune disruption of CD28, CTLA-4, or CD80 and/or CD86 have been shown to attenuate transplant rejection, autoimmune arthritis, and experimental allergic encephalitis. The use of CTLA-4 Ig, which reduces costimulation by binding to CD80 and CD86, has been shown to be protective in humans with type 1 diabetes by slowing the rate of β-cell loss when administered at an early stage of the disease. Unexpectedly, in this study, we observed an enhanced adipose inflammation and IR in mice deficient for CD80/CD86 despite decreased T-cell activation in circulation.

To investigate the role of costimulatory molecules CD80 and CD86 in obesity, human VAT and SAT derived from lean as well as obese/insulin-resistant humans were used for the detection of CD80 and CD86 on APCs. The obese adipose samples were obtained from obese patients undergoing endoscopic gastric bypass surgery. Most of the obese patients were on antidiabetic medication due to morbid obesity and the blood glucose and HbA_{1c} level was controlled in a relatively normal range. Despite

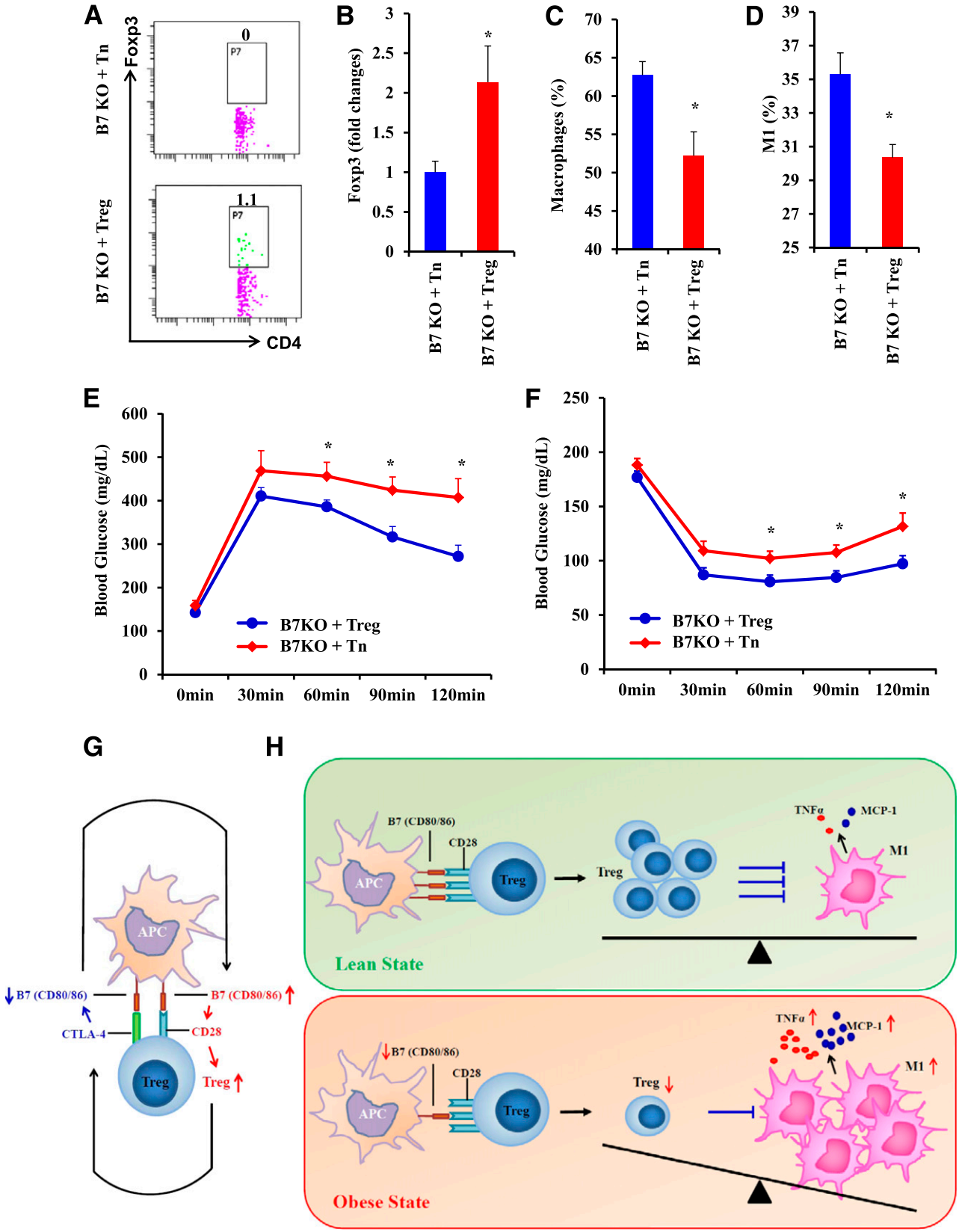

Figure 8—Adoptive transfer of Treg restores insulin sensitivity in B7 KO mice. Treg or Tn isolated from Foxp3-GFP knock-in mice were adoptively transferred into HF-fed B7 KO mice every other week. Adipose inflammation and IR were evaluated after 12 weeks. *A*: Presence of transferred Treg ($CD4^+GFP^+$) in SVF of mice transferred with Tregs but not those transferred with Tn. *B*: Epididymal fat was used for the real-time PCR analysis of Foxp3 expression. *C*: Macrophage ($CD11b^+$) infiltration in VAT of B7 KO mice transferred with Treg or Tn was evaluated by flow cytometry. *D*: Classical activation of ATM ($CD11c^+$ $CD11b^+$) was detected in VAT of B7 KO mice transferred with Treg of

relatively normal metabolic parameters in those obese patients, a correlation between B7 expression and degree of IR was observed. Further studies are required to confirm the implication of B7 in IR in humans. Despite higher indices of innate and adaptive immune inflammation, macrophages expressing $CD80^+CD86^+$ were decreased in both VAT and SAT compartments of obese patients, as well as in the VAT of HF-fed mice. A trend toward a decrease in CD80 and CD86 single positive cells was also noted, although no statistical significance was observed due to the relatively limited sample size. Further study is required to address the significance of CD80 and CD86 single positive cells. CD80/CD86 may be expressed in alternate cell types such as adipocytes and endothelial cells. The expression of CD80/CD86 on endothelial cells is typically low under unstimulated conditions (28) and is insufficient to activate T-cells (29). Since adipocytes constitute dominant cells in adipose, we investigated the expression in these cells and did not find a difference. Therefore, the expression of CD80/CD86 on macrophages, the dominant APCs in adipose tissue, may play an essential role in regulating costimulatory signaling of adipose tissue. Expression of CD80 and CD86 on macrophages in human VAT but not SAT was negatively correlated with HOMA-IR, suggesting a potential role of costimulation in IR. Consistent with our expectation that CD80/CD86 deletion would reduce T-cell activation, we observed reduced T-cell numbers and T-cell activation in CD80/CD86 B7 KO mice (7,10). Due to defective B7-mediated costimulation, T-cell numbers reduced in both spleen and adipose tissue. However, in contrast to our expectation, multiple measures of glucose/insulin homeostasis were impaired by deficiency of B7, despite lack of change in overall body weight and lower visceral adiposity. Since innate immune activation and inflammation are major drivers of IR and metabolic derangement (30–33), we observed an increased level of TNFα and MCP-1, as well as macrophage infiltration in VAT of both obese mice and obese humans.

Prior studies have implicated CD28 and CTLA-4 in Treg development (34–36). Blocking the B7/CD28 axis by neutralizing antibodies or CTLA-4 Ig reduced Treg in C57BL/6 and NOD mice (34,35). Using a CD80/CD86 B7 KO model, we provide direct evidence supporting the essential role of the B7/CD28 axis in Treg development and proliferation in this study. Tregs in spleen, blood, lymph nodes, as well as VAT were dramatically reduced in B7 KO mice. More importantly, a positive correlation between B7 expression on ATM and adipose-tissue-resident Treg was noted in human VAT samples. During the development of obesity, it has been suggested that there is a shift to proinflammatory M1-type macrophages, which contributes to IR. Tregs play an important role in maintaining immune balance by interacting with inflammatory cells, including T-cells and APCs (37). By coculturing Treg or Tn with macrophages, we confirmed that Treg suppresses $CD11c^+$ macrophage, a proinflammatory subpopulation of macrophage contributing to obesity-induced complications, including IR. In human VAT samples, we also observed a negative association between Treg and $CD11c^+CD11b^+$ cells. Consistent with this, the $CD11c^+CD11b^+$ population significantly decreased in VAT of B7 KO mice. Furthermore, adoptive transfer of Treg to B7 KO mice abrogated the increase of both macrophage infiltration and macrophage classical activation in VAT.

We next demonstrated that B7-deficient APCs displayed a reduced ability to promote Treg proliferation, differentiation from thymocytes, and conversion from $Foxp3^-$ T-cells. Moreover, Treg cocultured with $B7^{-/-}$ APCs has decreased suppressive functions, indicating that B7-mediated costimulation is essential for the differentiation, expansion, as well as function of Treg. Furthermore, Treg transfer restored insulin sensitivity and reduced macrophage-mediated adipose inflammation in B7 KO mice. It has been reported that Treg downregulates CD80 and CD86 on APCs through CTLA-4-mediated transendocytosis (38). On the basis of our observations, we propose a bidirectional control loop between Treg and B7 molecules on APCs in healthy individuals with prevention of excessive T-cell activation (Fig. 8*G*). In obese patients, it is likely that this feedback control loop between Treg and B7 molecules is impaired, leading to a progressive decrease of B7 and Treg, which enhances adipose inflammation (Fig. 8*H*). Our results do not provide insights on the primacy of each pathway or whether a decrease in CD80/CD86 occurs earlier in obesity than perturbations in Treg numbers. However, our results in ND-fed animals suggest that disruption of CD80/CD86 may alter Treg numbers/function even in the absence of HF diet.

Understanding the mechanisms underlying obesity-induced inflammation and IR is of critical importance in designing novel therapeutic approaches for the treatment of type 2 diabetes. In the current study, we demonstrate for the first time that CD80 and CD86 on ATM are essential in sustaining immune balance in adipose tissue. Expression

Tn. *E*: Levels of blood glucose were measured after intraperitoneal challenge of glucose (IPGTT). *F*: Levels of blood glucose after intraperitoneal challenge of insulin (ITT). $n = 5$ per group. *G*: Hypothetical model of negative feedback of B7 and Treg in healthy individuals. B7 on APCs promotes Treg proliferation and differentiation via interaction with CD28. CTLA-4 on Treg downregulates B7 expression on APCs. *H*: In lean humans, B7 expression on adipose resident APCs enhances Treg proliferation and differentiation. Treg subsequently suppresses $CD11c^+$ $CD11b^+$ cells and production of inflammatory cytokines such as TNFα and MCP-1. In obesity/IR, B7 reduced on adipose resident APCs, which results in reduced Treg and enhanced macrophage-mediated adipose inflammation. M1, classically activated macrophage. $^*P < 0.05$.

of CD80 and CD86 decreased during obesity and may represent an important mechanism of impaired Treg homeostasis in obese patients. Our results may have implications for therapies that target costimulation for the treatment of type 2 diabetes and suggest that their application may need to consider potential adverse consequences on Tregs.

Acknowledgments. The authors thank Randy Seeley, University of Cincinnati College of Medicine, for valuable suggestions on the manuscript.

Funding. This work was supported by R01-ES-015146, R01-ES-017290, R21-HL-108467, and R21-DK-088522. J.Z. was supported by RC063384OSU, 13POST17210033, and 81101553. J.A.D. was supported by a National Research Service Award (F32-DK-083903).

Duality of Interest. No potential conflicts of interest relevant to this article were reported.

Author Contributions. J.Z. researched data and wrote the manuscript. X.R. and Z.B. researched data. A.T., V.N., J.H., D.M., B.N., J.R., and J.A.D. contributed to clinical tissue collection. Q.S. and A.R.S. contributed to discussion. S.R. reviewed and edited the manuscript. J.Z. is the guarantor of this work and, as such, had full access to all the data in the study and takes responsibility for the integrity of the data and the accuracy of the data analysis.

References

1. Hotamisligil GS. Inflammation and metabolic disorders. Nature 2006;444:860–867
2. Després JP, Lemieux I. Abdominal obesity and metabolic syndrome. Nature 2006;444:881–887
3. Horng T, Hotamisligil GS. Linking the inflammasome to obesity-related disease. Nat Med 2011;17:164–165
4. Feuerer M, Herrero L, Cipolletta D, et al. Lean, but not obese, fat is enriched for a unique population of regulatory T cells that affect metabolic parameters. Nat Med 2009;15:930–939
5. Nishimura S, Manabe I, Nagasaki M, et al. CD8+ effector T cells contribute to macrophage recruitment and adipose tissue inflammation in obesity. Nat Med 2009;15:914–920
6. Sell H, Habich C, Eckel J. Adaptive immunity in obesity and insulin resistance. Nat Rev Endocrinol 2012;8:709–716
7. Smith-Garvin JE, Koretzky GA, Jordan MS. T cell activation. Annu Rev Immunol 2009;27:591–619
8. McAdam AJ, Schweitzer AN, Sharpe AH. The role of B7 co-stimulation in activation and differentiation of CD4+ and CD8+ T cells. Immunol Rev 1998;165:231–247
9. Harris NL, Ronchese F. The role of B7 costimulation in T-cell immunity. Immunol Cell Biol 1999;77:304–311
10. Lenschow DJ, Walunas TL, Bluestone JA. CD28/B7 system of T cell costimulation. Annu Rev Immunol 1996;14:233–258
11. Girvin AM, Dal Canto MC, Rhee L, et al. A critical role for B7/CD28 costimulation in experimental autoimmune encephalomyelitis: a comparative study using costimulatory molecule-deficient mice and monoclonal antibody blockade. J Immunol 2000;164:136–143
12. Judge TA, Wu Z, Zheng XG, Sharpe AH, Sayegh MH, Turka LA. The role of CD80, CD86, and CTLA4 in alloimmune responses and the induction of long-term allograft survival. J Immunol 1999;162:1947–1951
13. O'Neill SK, Cao Y, Hamel KM, Doodes PD, Hutas G, Finnegan A. Expression of CD80/86 on B cells is essential for autoreactive T cell activation and the development of arthritis. J Immunol 2007;179:5109–5116
14. Racke MK, Scott DE, Quigley L, et al. Distinct roles for B7-1 (CD-80) and B7-2 (CD-86) in the initiation of experimental allergic encephalomyelitis. J Clin Invest 1995;96:2195–2203
15. Stumpf M, Zhou X, Bluestone JA. The B7-independent isoform of CTLA-4 functions to regulate autoimmune diabetes. J Immunol 2013;190:961–969
16. Tellander AC, Pettersson U, Runström A, Andersson M, Michaëlsson E. Interference with CD28, CD80, CD86 or CD152 in collagen-induced arthritis. Limited role of IFN-gamma in anti-B7-mediated suppression of disease. J Autoimmun 2001;17:39–50
17. Vinh A, Chen W, Blinder Y, et al. Inhibition and genetic ablation of the B7/CD28 T-cell costimulation axis prevents experimental hypertension. Circulation 2010;122:2529–2537
18. Zhong J, Rao X, Deiuliis J, et al. A potential role for dendritic cell/macrophage-expressing DPP4 in obesity-induced visceral inflammation. Diabetes 2013;62:149–157
19. Shah Z, Kampfrath T, Deiuliis JA, et al. Long-term dipeptidyl-peptidase 4 inhibition reduces atherosclerosis and inflammation via effects on monocyte recruitment and chemotaxis. Circulation 2011;124:2338–2349
20. Zhong J, Yang P, Muta K, et al. Loss of Jak2 selectively suppresses DC-mediated innate immune response and protects mice from lethal dose of LPS-induced septic shock. PLoS ONE 2010;5:e9593
21. Rached MT, Kode A, Silva BC, et al. FoxO1 expression in osteoblasts regulates glucose homeostasis through regulation of osteocalcin in mice. J Clin Invest 2010;120:357–368
22. Hsieh CS, Lee HM, Lio CW. Selection of regulatory T cells in the thymus. Nat Rev Immunol 2012;12:157–167
23. Martín-Gayo E, Sierra-Filardi E, Corbí AL, Toribio ML. Plasmacytoid dendritic cells resident in human thymus drive natural Treg cell development. Blood 2010;115:5366–5375
24. Denning TL, Wang YC, Patel SR, Williams IR, Pulendran B. Lamina propria macrophages and dendritic cells differentially induce regulatory and interleukin 17-producing T cell responses. Nat Immunol 2007;8:1086–1094
25. Kushwah R, Hu J. Role of dendritic cells in the induction of regulatory T cells. Cell Biosci 2011;1:20
26. Bilate AM, Lafaille JJ. Induced CD4+Foxp3+ regulatory T cells in immune tolerance. Annu Rev Immunol 2012;30:733–758
27. Olefsky JM, Glass CK. Macrophages, inflammation, and insulin resistance. Annu Rev Physiol 2010;72:219–246
28. Hancock WW, Sayegh MH, Zheng XG, Peach R, Linsley PS, Turka LA. Costimulatory function and expression of CD40 ligand, CD80, and CD86 in vascularized murine cardiac allograft rejection. Proc Natl Acad Sci U S A 1996;93:13967–13972
29. Katz SC, Pillarisetty VG, Bleier JI, Shah AB, DeMatteo RP. Liver sinusoidal endothelial cells are insufficient to activate T cells. J Immunol 2004;173:230–235
30. Hotamisligil GS, Shargill NS, Spiegelman BM. Adipose expression of tumor necrosis factor-alpha: direct role in obesity-linked insulin resistance. Science 1993;259:87–91
31. Kanda H, Tateya S, Tamori Y, et al. MCP-1 contributes to macrophage infiltration into adipose tissue, insulin resistance, and hepatic steatosis in obesity. J Clin Invest 2006;116:1494–1505
32. Shoelson SE, Lee J, Goldfine AB. Inflammation and insulin resistance. J Clin Invest 2006;116:1793–1801
33. Xu H, Barnes GT, Yang Q, et al. Chronic inflammation in fat plays a crucial role in the development of obesity-related insulin resistance. J Clin Invest 2003;112:1821–1830
34. Tang Q, Henriksen KJ, Boden EK, et al. Cutting edge: CD28 controls peripheral homeostasis of CD4+CD25+ regulatory T cells. J Immunol 2003;171:3348–3352
35. Walker LS, Sansom DM. The emerging role of CTLA4 as a cell-extrinsic regulator of T cell responses. Nat Rev Immunol 2011;11:852–863
36. Salomon B, Lenschow DJ, Rhee L, et al. B7/CD28 costimulation is essential for the homeostasis of the CD4+CD25+ immunoregulatory T cells that control autoimmune diabetes. Immunity 2000;12:431–440
37. Fehérvari Z, Sakaguchi S. CD4+ Tregs and immune control. J Clin Invest 2004;114:1209–1217
38. Qureshi OS, Zheng Y, Nakamura K, et al. Trans-endocytosis of CD80 and CD86: a molecular basis for the cell-extrinsic function of CTLA-4. Science 2011;332:600–603